

**High Spatial Resolution Grain Orientation and Strain  
Mapping in Thin Films using Polychromatic  
Submicron X-ray Diffraction**

N. Tamura *et al.*

---

*Stanford Linear Accelerator Center, Stanford University, Stanford, CA 94309*

Work supported by Department of Energy contract DE-AC03-76SF00515.

# High Spatial Resolution Grain Orientation and Strain Mapping in Thin Films using Polychromatic Submicron X-ray Diffraction

N. Tamura, A.A.MacDowell, R. S. Celestre, H.A. Padmore,

*Advanced Light Source, 1 Cyclotron Road, Berkeley CA 94720*

B. Valek, J. C. Bravman

*Dept. Materials Science & Engineering, Stanford University, Stanford CA 94305*

R. Spolenak, W.L. Brown

*Agere Systems, formerly Bell Laboratories, Lucent Technologies, Murray Hill NJ 07974*

T.Marieb, H. Fujimoto

*Intel Corporation, Santa Clara CA 95052, and Intel Corporation, Portland, OR 97124*

B.W. Batterman, J. R. Patel

*Advanced Light Source, 1 Cyclotron Road, Berkeley CA 94720, and Stanford*

*Synchrotron Radiation Laboratories, P.O.BOX 4349, Stanford CA 94309*

## ABSTRACT:

The availability of high brilliance synchrotron sources, coupled with recent progress in achromatic focusing optics and large area 2D detector technology, have allowed us to develop a X-ray synchrotron technique capable of mapping orientation and strain/stress in polycrystalline thin films with submicron spatial resolution. To demonstrate the capabilities of this instrument, we have employed it to study the microstructure of aluminum thin film structures at the granular and subgranular level. Owing to the relatively low absorption of X-rays in materials, this technique can be used to study passivated samples, an important advantage over most electron probes given the very different mechanical behavior of buried and unpassivated materials.

Deposited metal thin films patterned into micron-scale structures are ubiquitous in integrated circuits and other modern technologies<sup>1</sup>. Working with laboratory X-ray sources many authors<sup>2,3,4</sup> have provided valuable information on the average behavior of thin films obtained over a length scale of millimeters. Individual grains in such films are usually in the micron size range, a thousand times smaller than the spatial resolution available with laboratory x-ray instruments. In this letter, we describe the application of a technique using submicron synchrotron-based X-ray diffraction, developed at the Advanced Light Source, to characterize both the orientation and strain/stress state of blanket thin films and patterned, passivated interconnect lines, including the change in stress state as they undergo thermal cycling. Similar or related techniques have also been developed at other synchrotron facilities to measure strain in Al interconnect lines<sup>5,6,7</sup>.

There are many ways<sup>8</sup> to produce x-ray microbeams. Our technique requires white instead of monochromatic radiation to rapidly determine the orientation of each illuminated grain by taking a Laue pattern in reflection mode. To form the required high quality white light focus, we use a pair of orthogonal elliptical Kirkpatrick-Baez (KB) mirrors<sup>9,10,11</sup> in grazing incidence for point to point imaging. The elliptical shape of our KB mirrors are produced by controlled bending of a flat substrate, which has a specific width variation allowing us to generate a 0.8 x 0.7  $\mu\text{m}$  white X-ray beam by demagnifying a bending magnet synchrotron radiation source<sup>10</sup>.

Each Laue pattern is recorded with a large area X-ray charge coupled device (CCD) camera. Custom software based on previous algorithms<sup>12</sup> permits us to rapidly index the white-beam

Laue spots and to calculate orientation matrices even if multiple grains are illuminated. Additionally, by measuring the deviations of the Laue spot positions from those predicted for the ideal unstrained crystal structure, the complete deviatoric (distortional) strain tensor of the illuminated volume can be computed. For cubic crystals, knowledge of the magnitude of the unstrained lattice parameter is in general unnecessary. The stress tensor is calculated from the strain tensor using the anisotropic elastic constants of the material. Complete maps of the orientation and deviatoric stress/strain tensors are obtained by scanning the sample beneath the focused white beam and recording a Laue pattern at each step. A high-resolution grain map is obtained by extracting the intensity profile of each individual grain from the Laue diffraction scan. The contours of the grain boundaries are interpolated by intersecting the resulting normalized intensity profiles.

The samples investigated are sputtered Al (0.5 wt.% Cu) thin film test structures designed for electromigration studies. The patterned lines, passivated with 0.7  $\mu\text{m}$  of  $\text{SiO}_2$  (PETEOS), have dimensions 0.7 or 4.1  $\mu\text{m}$  in width, 30  $\mu\text{m}$  in length and 0.75  $\mu\text{m}$  in thickness. Ti shunt layers are present at the bottom and the top of the lines. A 100 x 100  $\mu\text{m}$  bond pad on the chip with a thin Ti underlayer is used to simulate a bare blanket film.

An example of a Laue pattern obtained by this X-ray microdiffraction technique is shown in Fig. 1. In the raw data (Fig. 1(a)), reflections from the Si substrate dominate. The Si pattern is digitally subtracted to obtain the indexed Al grain Laue pattern of Fig. 1(b). Note that the (333) Al spot equivalent to the [111] direction is close to the center of the pattern, which approximately represents the normal to the (001) silicon surface. A grain map showing the in

plane orientation of a 0.7  $\mu\text{m}$  wide test interconnect line is shown in Fig. 1(c). The pole figure shows a preferred (111) out of plane texture within  $3^\circ$  of the surface normal. The grain map of the 0.7  $\mu\text{m}$  line in Fig. 1(c) shows the typical bamboo structure expected from narrow lines where individual grains span the width of the line.

A grain orientation map for a wider 4.1  $\mu\text{m}$  passivated Al(Cu) line is shown in Fig 2. Since the grain size of the deposited film is about 1  $\mu\text{m}$ , the 4.1  $\mu\text{m}$  line has multiple grains across its width. The variation of the in plane and out of plane grain orientation is similar to that for the 0.7  $\mu\text{m}$  line. The diagonal components of the deviatoric or distortional stress tensor  $\sigma_{xx}'$ ,  $\sigma_{yy}'$ ,  $\sigma_{zz}'$  are shown in Fig. 2(b). The stress state in these films is far from homogeneous and appreciable local stress gradients exist.

In Fig. 3, we show the orientation map for a  $5 \times 5 \mu\text{m}$  region of a bare bond pad, the equivalent of a blanket thin film. As in the previous cases the out of plane (111) orientation varies from  $0 - 3^\circ$ . It is evident that on the local microscopic level the deviatoric stresses  $\sigma_{xx}' \neq \sigma_{yy}'$ . Our data indicate that in polycrystalline blanket films the local stress is generally very different from the average stress. In particular, at the granular and subgranular level, the stress can depart significantly from biaxiality. However, if we average the data over the  $5 \times 5 \mu\text{m}$  scanned area, we retrieve the biaxiality i.e.:  $\langle \sigma_{xx}' \rangle \approx \langle \sigma_{yy}' \rangle$ . The average biaxial stress of the film can be computed assuming that the out-of-plane average total stress  $\langle \sigma_{zz}' \rangle = 0$ . Expressing the total average stress matrix as the sum of the deviatoric and hydrostatic stress components one can show that the average biaxial stress  $\langle \sigma_b \rangle = \langle \sigma_{xx}' \rangle = \langle \sigma_{yy}' \rangle = \langle \{(\sigma_{xx}' + \sigma_{yy}')/2\} - \sigma_{zz}' \rangle$ . The average biaxial stress in the example above was 68 MPa. The low room temperature value of this

stress is due to relaxation over time for this particular sample. In order to eliminate relaxation effects the sample was heated to 400° C, and cooled to room temperature before the thermal cycle experiment described below.

A plot of the average biaxial stress in the film obtained by x-ray microdiffraction during a thermal cycle between 25°C and 345°C is shown in Fig. 4. The stresses in approximately 130 grains in a 15µm x 15µm region were averaged to give the results shown in the figure. Though our temperature range is about 100°C smaller, the temperature cycling curve using microdiffraction is very similar to that reported by Venkatraman et al<sup>13</sup> using wafer curvature measurements on an Al(Cu) films with thickness 1 µm. The film is in tension at room temperature, with an average biaxial stress of 230 MPa. The measured stress is caused by mismatch between the thermal expansion coefficients of the aluminum and the silicon substrate. Upon heating, the higher thermal expansion coefficient of the aluminum film relaxes the tensile stress before driving the film into compression. From Fig. 4 the experimentally determined initial thermoelastic slope is  $(d\sigma / dT) = 2.53 \text{ MPa} / ^\circ\text{C}$ . The theoretical thermoelastic slope can be calculated from the relation  $(d\sigma / dT) = \Delta\alpha M(111)$ , where the biaxial modulus<sup>14</sup> for a highly textured (111) Al film is  $M(111) = 6C_{44}(C_{11} + 2C_{12}) / (C_{11} + 2C_{12} + 4C_{44}) = 114 \text{ GPa}$ . From which we obtain  $(d\sigma / dT) = 2.34 \text{ MPa} / ^\circ\text{C}$ , in reasonable agreement with the experimental value.

Our X-ray microdiffraction technique gives results on average consistent with those from conventional macroscopic probes, but its real advantage lies in the fact that it also provides information at a very local level, allowing the study of mechanical properties of thin films in new detail. For instance, the point in the thermal cycle curve where the initial slope of the heating

cycle departs from linearity is frequently regarded as the yield stress of the film. While this may be in fortuitous agreement with the flow stress in some cases this cannot in general be true. It is evident from the work of Venkatraman et al.<sup>13</sup> and our results in Fig. 4 that the yield stress based on the above criterion is in the vicinity of 0 MPa. Thus the departure from linearity for the initial slope during the heating cycle cannot be correctly interpreted as always representing the plastic flow stress in the film. A more likely explanation emerges from our detailed measurements of the local stress distribution in the film. At room temperature, the stress is highly inhomogeneous with regions sustaining more tensile stress than others. Upon heating some regions of the film become compressive while the average biaxial stress is still in the tensile regime. Even though the average stress is zero at about 100°C some grains have already reached their yield stress and deformed and the heating curve departs from linearity. The temperature at which the curve departs from linearity is quite variable for different films and depends on detailed process parameters.

In summary we have demonstrated the versatility of the X-ray Microdiffraction facility at the Advanced Light Source (ALS) in providing detailed microscopic information on the properties of thin polycrystalline films. Further development of the submicron X-ray diffraction technique should provide useful information on the behavior of materials at the micron and submicron level. Microscopic knowledge of the local orientation and strain state parameters will broadly enhance our understanding of the complex and intricate links between the macroscopic and the microscopic properties of thin films as well as bulk polycrystalline materials.

#### ACKNOWLEDGEMENTS



The Advanced Light Source is supported by the Director, Office of Science, Office of Basic Energy Sciences, Materials Sciences Division, of the U.S. Department of Energy under Contract No. DE-AC03-76SF00098 at Lawrence Berkeley National Laboratory. We also thank John Carruthers and Intel Corporation for encouragement and generous help towards instrumenting the Microdiffraction beamline.

## REFERENCES:

1. J. D. Plummer, M. D. Deal, P. B. Griffin, *Silicon VLSI Technology Fundamentals, Practice and Modeling*, (Prentice Hall, Upper Saddle River, NJ, 2000)
2. A. Seegmuller and M. Murakami, *Treatise on Materials Science and Engineering, Vol. 27*, H. Herman Ed. Academic Press, New York, 1988, pp.143-200.
3. P. A. Flinn and G. A. Waychunas, *J. Vac. Sci. & Tech.* **B6**, 1749 (1988).
4. P. A. Flinn and C. Chiang, *J. Appl. Phys.* **67**, 2927 (1990)
5. P. C. Wang, G. S. Cargill III, I. C. Noyan and C. K. Hu, *Appl. Phys. Lett.* **72**, 1296 (1998).
6. N. Tamura, J.-S. Chung, G. E. Ice, B. C. Larson, J. D. Budai, J. Z. Tischler, M. Yoon, E.L. Williams, and W. P. Lowe, *Mater. Res. Soc. Symp. Proc*, **563**, 175 (1999).
7. P.-C. Wang, I. C. Noyan, S. K. Kaldor, J. L. Jordan-Sweet, E. G. Liniger, and C.-H. Ku, *Appl. Phys. Lett.*, **78**, 2712 (2001).
8. G. E. Ice, *X-ray Spectrometry* (2001) To be published.
9. G. E. Ice, J.-S. Chung, J. Z. Tischler, A. Lunt and L. Assoufid, *Rev. Sci. Inst.* **71**, 2635 (2000)
10. A. A. MacDowell, R. S. Celestre, N. Tamura, R. Spolenak, B. C. Valek, W. L. Brown, J. C. Bravman, H. A. Padmore, B. W. Batterman, and J. R. Patel, *Nucl. Instr. & Meth. In Phys. Res. A* **467-468**, 936 (2001).

11. O. Hignette, G. Rostaing, P. Cloetens, A. Rommeveaux, W. Ludwig, and A. Freund, SPIE Conf. Proc. 4499 (San Diego, 2001) To be published.
12. J.-S. Chung and G.E. Ice, J. Appl. Phys., **86**, 5249 (1999)
13. R. Venkatraman, J. C. Bravman, W. D. Nix, P. W. Davies, P. A. Flinn, D. B. Fraser. J. of Electron. Matls. **19**, 1231 (1990).
14. W. D. Nix, Metall. Trans. A, **20A**, 2217 (1989).

## FIGURE CAPTIONS

Figure 1. (a) Laue pattern from a 0.7  $\mu\text{m}$  wide passivated Al(Cu) line showing both the substrate Si and Al(Cu) grain spots (b) indexed Al(Cu) Laue pattern, the Si substrate peaks have been subtracted. (c) Grain map and pole figure showing the [111] directions of all grains along a 30  $\mu\text{m}$  length Al(Cu) line.

Figure 2. (a) Grain map of a 4.1  $\mu\text{m}$  passivated Al(Cu) interconnect line. (b) Local x, y, and z diagonal components of the measured deviatoric (distortional) stress tensor showing inhomogeneous stress distribution. The x-axis is along the length of the line, the y-axis is across the line, and the z-axis is normal to the sample surface. The  $\sigma_{xx}'$  component along the line is mainly positive, varying from about -15 MPa to about +60 MPa. Across the sample the  $\sigma_{yy}'$  component is predominantly negative varying from -50 to +20 MPa, while in the  $\sigma_{zz}'$  direction except for a small +40 MPa region the stresses vary from -20 MPa to about +30 MPa.

Figure 3. (a) Grain Map of a 5  $\mu\text{m} \times 5 \mu\text{m}$  unpassivated blanket Al(Cu) film. (b) Local deviatoric stress maps of the diagonal components of the stress tensor. Both  $\sigma_{xx}'$  and  $\sigma_{yy}'$  lie between 0 and +60 MPa.  $\sigma_{zz}'$  varies from -65 to 0 MPa.

Figure 4. Thermal cycling results on a 15 $\times$ 15  $\mu\text{m}$  area of an Al(Cu) bond pad (blanket film) showing the averaged biaxial stress component  $\langle \sigma_b \rangle$  versus temperature. The insets show detailed stress distribution in the film at different temperatures (The 2D maps are a plot of  $-\sigma_{zz}' = \sigma_{xx}' + \sigma_{yy}'$  as a measure of the in-plane stress). Note the blue regions of compressive stress in the 105  $^\circ\text{C}$  map, while on average the stress is still in the tensile regime.

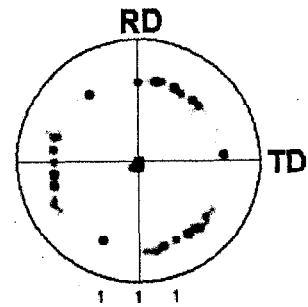
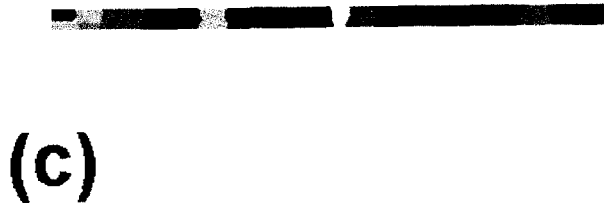
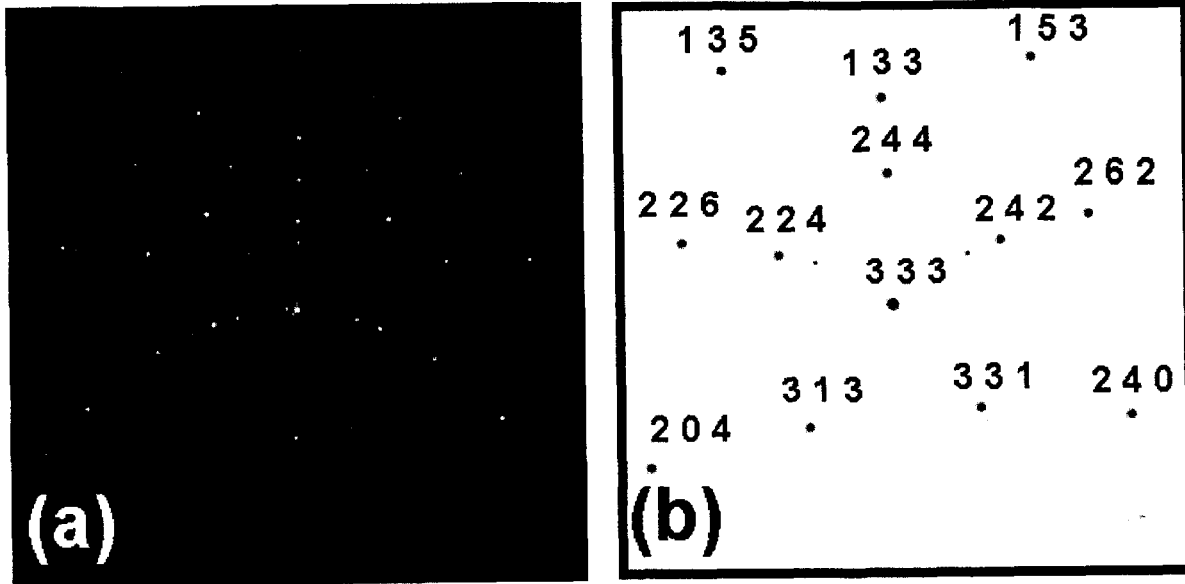


Fig 1. N. Tamura et al.,

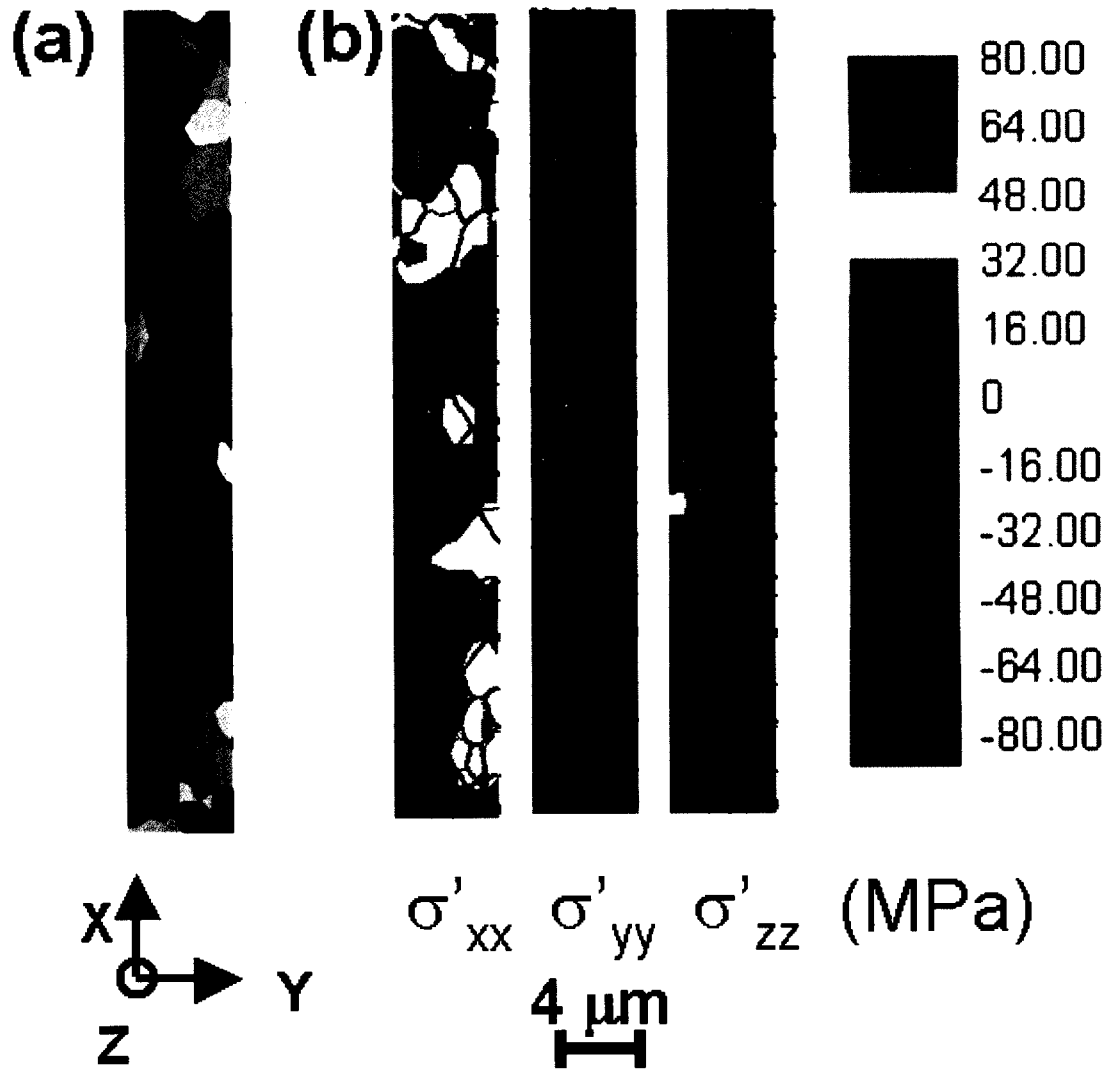


Fig 2., N. Tamura et al.

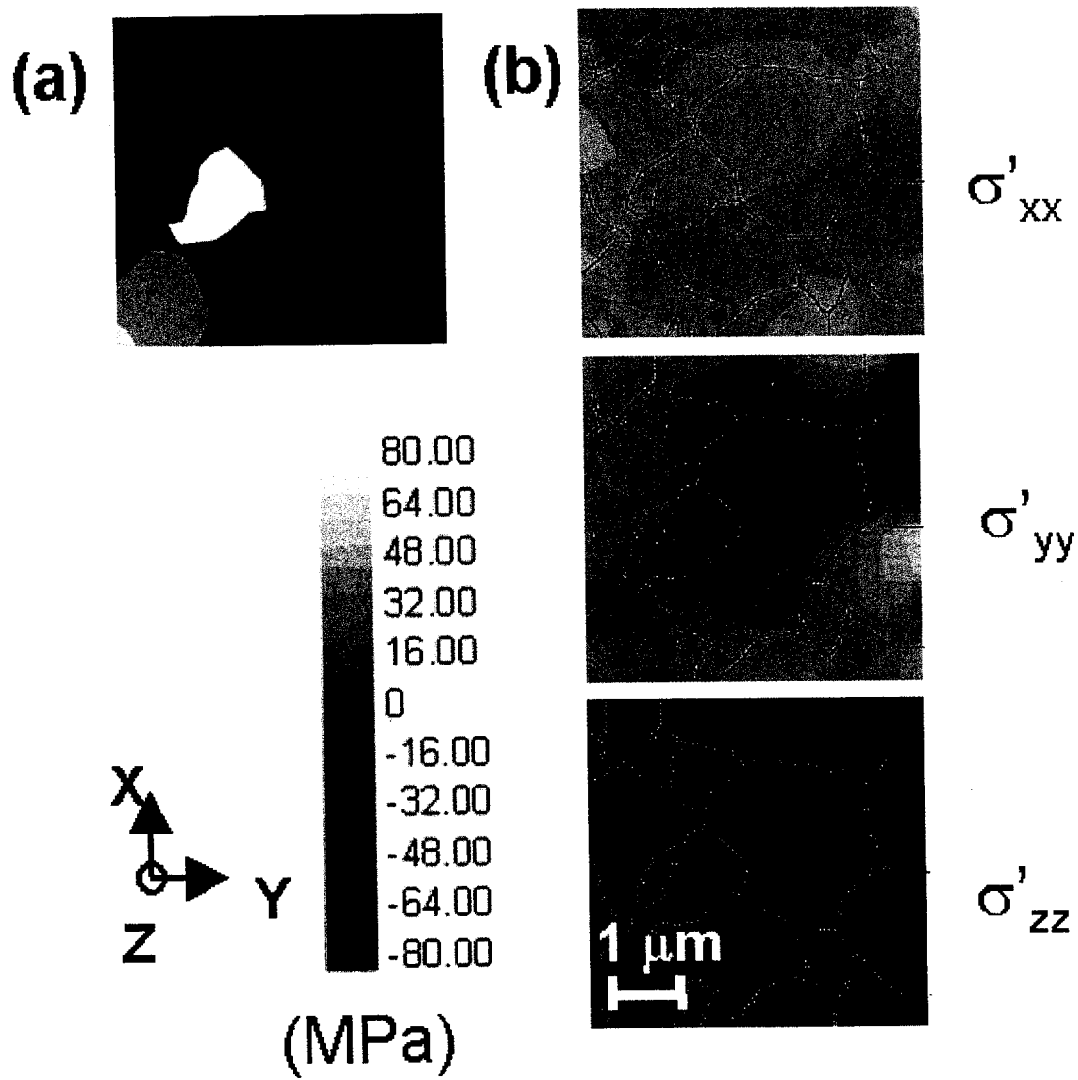


Fig. 3, N. Tamura et al.

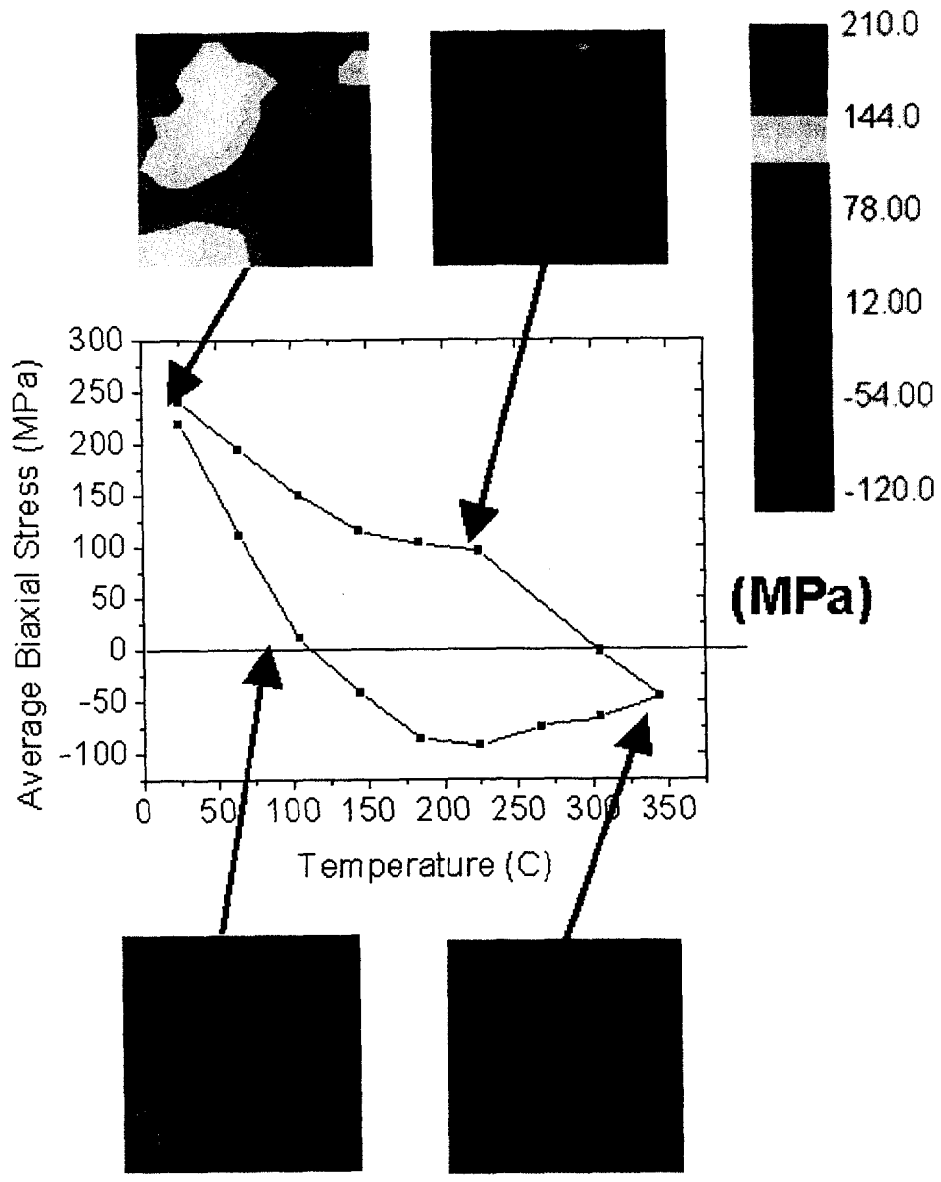


Fig. 4, N. Tamura et al.